MEASUREMENTS OF EMISSION TEMPERATURES FROM SHOCKED H_2O ICE. S. T. Stewart[1], A. Seifter[2], and A. W. Obst[2], [1]Harvard University, Department of Earth and Planetary Sciences, 20 Oxford St., Cambridge, MA 02138 (sstewart@eps.harvard.edu), [2]Los Alamos National Laboratory, Los Alamos, NM 87545.

Introduction: Impact cratering is one of the major geologic processes on the icy planets and satellites in the outer solar system. The outcome of impact calculations have been used to suggest the presence of transient liquid water [1-3] and to infer the thickness of brittle crusts [4]. These studies rely on the model equation of state of H_2O to infer the post-impact temperature field and the occurrence of phase changes. However, no experimental data had been collected on the shock temperature of ice to validate the equations of state models. Here, we present results from the first shock pyrometry experiments on H_2O ice.

Experiments. Specimens of polycrystalline S2 columnar ice are grown from distilled water in a subzero laboratory. Samples are cored in the columnar direction and cut into nominally Ø31×3 mm discs. The typical grain size is 3-4 mm. Specimens are grown slowly to allow outgassing of trapped air, and no bubbles are observed under microscopic examination.

Planar shock waves, with peak pressures up to ~15 GPa, are generated in ice using the 40-mm single stage powder gun in the Harvard Shock Compression Laboratory [5]. Simultaneous particle velocity and radiance measurements are recorded from the downrange face of the samples. Samples are mounted on an Al driver plate and enclosed in an ~1 microtorr vacuum chamber [6, 7]. The driver plates are lapped plane parallel and polished to an optical (~100 nm) finish so that they have a negligble contribution to the observed emission [6]. The ice is hand lapped and polished to a several 100's nm finish.

The initial sample temperature must be below -100 ºC to avoid significant sublimation under vacuum. Target assemblies are cooled by circulating liquid nitrogen through the driver plate. The ice is affixed mechanically and conductively cooled by the driver plate. The CaF_2 viewing window on the downrange face of the target vacuum chamber is actively heated to prevent frosting.

Time-resolved emission is collected by a 0.65-μm photomultiplier tube and a high-speed, infrared (IR), four-wavelength (1.8, 2.3, 3.5, 4.8 μm) pyrometer [8]. The IR pyrometer is sensitive to radiance temperatures as low as 400 K and has a temporal resolution of ~17 ns. The pyrometer viewing area is ~4-mm diameter at the focal distance of the optics. The viewing area increases when the sample is brought into motion by the shock wave. Free surface particle velocities are recorded by a Valyn Velocity Interferometer for Any Reflector (VISAR).

Because the emissivity of ice is nearly one, no emissivity correction is applied to the observed radiation temperature. If the observed temperature at all wavelengths are equal, then it is considered the true temperature of a homogeneous surface. If not, then the sample temperature is heterogeneous [7].

Results. Time histories of emission temperatures in ice record the peak shock temperature during passage of the shock wave through the sample and the final temperature after release to ambient conditions (Fig. 1). All of the features in the time resolved temperature record are reproducible. The observed emission is a strong function of wavelength because of the wavelength-dependent absorption of ice [9]. Therefore, no emission is seen at 3.5 or 4.8 μm until the shock wave nearly reaches the free surface, and the emission at these wavelengths never reaches the peak shock temperature.

A temperature spike is observed when the shock wave enters the ice because of the small gap, with possibly some trapped air, between the Al driver and the sample. The observed emission rises as the shock wave travels through the sample and the absorption length decreases. Just before the shock pressure is released from the free surface, the peak shock temperature is recorded. The coincidence of the 1.8 and 2.3 μm data records the true peak shock temperature.

After release to ambient conditions, the post-shock temperature follows a distribution typical of shocked natural materials [7, 10]: a heterogeneous temperature distribution characterized by a low continuum (bulk) temperature and a small area fraction of extremely hot material. In emission temperature measurements on basalt, hot spots were strongly correlated with pore spaces [10]. In the case of ice, the hot spots are likely caused by shearing at grain boundaries. The increasing temperature after the time of the minimum post-shock temperature is well modeled by the increasing area fraction of hot spots in the field of view, caused by the moving sample.

The visible wavelength channel is dominated by hot spots and appears to be overwhelmed by a miniscule fraction of very hot shocked air that has a negligible contribution to the infrared wavelengths. Attempts to model the passage of the shock wave through the sample to derive simultaneous emissivity and tempera-

ture using the method of [11] have been dissatisfactory, partly because only the 1.8 and 2.3 μm channels have a continuous record through the sample.

Measured continuum peak shock temperatures of 750 to 1000 K between 9-14 GPa are in excellent agreement with Hugoniot calculations by [12]. Post-shock continuum temperatures are 400-550 K. The ice has reached complete vaporization at much lower shock pressures than suggested by previous calculations, which estimated that shock pressures in excess of 50 GPa were required [12]. The discrepancy likely arises because the calculation assumes a constant specific heat capacity for H_2O over a wide range of pressures and temperatures. Calculations using a new tabular equation of state for H_2O ice (developed by Stewart for [13]) based on [12, 14-16] are in excellent agreement with the measured shock and post-shock temperatures.

Conclusions. Shock and post-shock temperature measurements in H_2O ice provide critical data for calculations of phase changes induced by impact events in the solar system. Heterogeneous temperature fields are observed in polycrystalline samples, implying high temperatures in shear zones along grain boundaries. The first shock temperature data collected on H_2O ice indicate that previous estimates of the shock pressures required for vaporization were much too high.

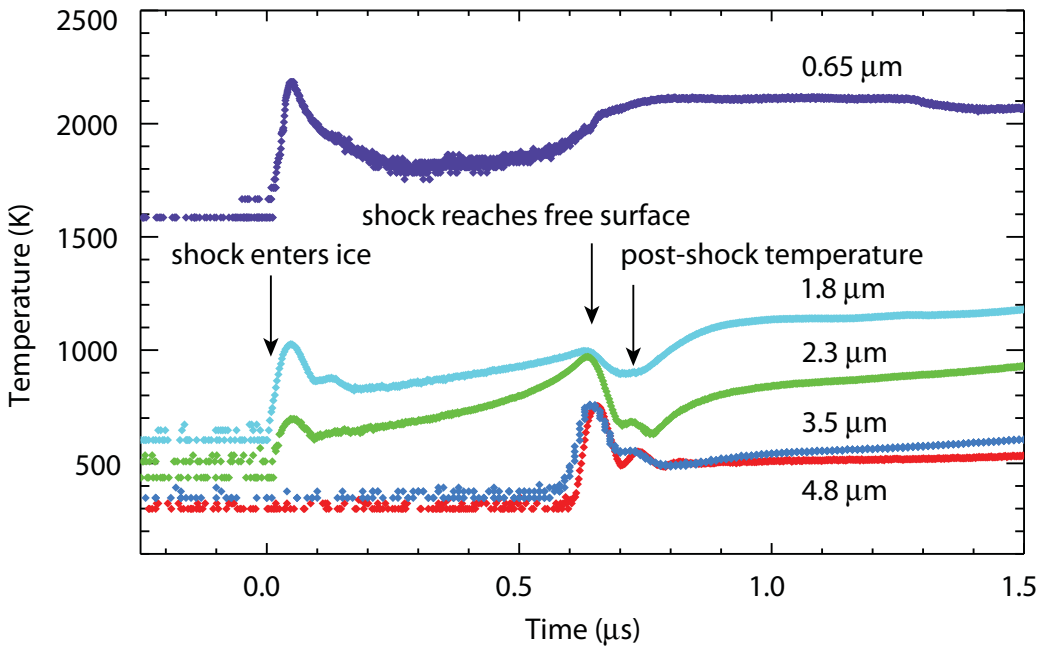

Figure 1. Pyrometery results for ice experiment with a peak shock pressure of 13.6 GPa.

References.
[1] Artemieva, N. and J.I. Lunine (2005) *Icarus* **175**(2), 522-533.
[2] Artemieva, N. and J. Lunine (2003) *Icarus* **164**(2), 471-480.
[3] Pierazzo, E., N.A. Artemieva, and B.A. Ivanov (2005) *Geological Society of America Special Paper* **384**, 443-457.
[4] Turtle, E.P. and E. Pierazzo (2001) *Science* **294**(5545), 1326-1328.
[5] Stewart, S.T. (2004) *LPSC* **35**, Abs. 1290.
[6] Seifter, A., et al. (2006) *Shock Compression of Condensed Matter -- 2005*, American Institute of Physics, p. 139-142.
[7] Stewart, S.T., et al. (2006) *Shock Compression of Condensed Matter -- 2005*, American Institute of Physics, p. 1484-1487.
[8] Boboridis, K., A. Seifter, and A.W. Obst (2003) *VDI-Bericht* **1784**, 119-126.
[9] Petrenko, V.F. and R.W. Whitworth (1999) *Physics of Ice*. New York: Oxford U. Press.
[10] Stewart, S.T., et al. (2007) *LPSC* **38**, Abs. 2413.
[11] Luo, S.N., et al. (2004) *JGR* **109**(B5).
[12] Stewart, S.T. and T.J. Ahrens (2005) *JGR* **110**, E03005.
[13] Leinhardt, Z.M. and S.T. Stewart (submitted) *Icarus*.
[14] Wagner, W. and A. Pruss (2002) *Journal of Physical and Chemical Reference Data* **31**(2), 387-535.
[15] Frank, M.R., Y.W. Fei, and J.Z. Hu (2004) *Geochimica et Cosmochimica Acta* **68**(13), 2781-2790.
[16] Feistel, R. and W. Wagner (2006) *Journal of Physical and Chemical Reference Data* **35**(2), 1021-1047.